Coherent excitation of cadmium $J=0,1,2$ autoionizing levels by electron impact

N. L. S. Martin and D. B. Thompson
Department of Physics and Astronomy, University of Kentucky, Lexington, Kentucky 40506-0055
(Received 4 September 1990)

We have measured $(e,2e)$ energy spectra in cadmium for the $4d^9 5s^2 5p\ J=1$ autoionizing region. The ejected-electron energy range investigated was from 2.6 to 4.8 eV with an incident electron energy of 150 eV and a scattering angle of 3°. Small differences were found in spectra taken at ejected-electron directions 180° apart. We ascribe these differences to interference terms arising from coherent excitation of the $J=1$ and overlapping $5pnp\ J=0,2$ autoionizing levels. A calculation of these effects is presented that agrees quite well with the experimental data. We obtain experimental excitation amplitude ratios and assign a previously undetected autoionizing level to $5p6p\ ^3D_2$.

I. INTRODUCTION

In a coherence experiment, the decay products of an intermediate excited state are detected. The state may be mathematically represented as a coherent superposition of basis states and the experiment is designed to enable both the magnitude and the relative phases of the basis-state coefficients to be determined.

The best-known experiments on collisionally induced coherence are those on the degenerate magnetic sublevels of the He $2\ ^1P$ state.[1] Similar experiments have been carried out on coherent excitation of the magnetic sublevels of a single autoionizing level.[2] In these experiments, angular distributions of either emitted photons or ejected electrons, measured in coincidence with scattered particles, yield relative excitation amplitudes and phases for the magnetic sublevels.

Little work has been done on collisionally induced coherences between states of different total angular momentum.[2] Such systems are of interest because they provide the next step in the test of scattering theories beyond that of the excitation of different sublevels of a single level. For autoionizing levels, if the separations of resonance maxima are comparable to the large widths associated with short-lived autoionizing states, interference between the excitation amplitudes will affect the overall line profiles and ejected-electron angular distributions. Such effects have been observed in ion-He and slow (i.e., close to threshold) electron-He collisions,[3] but in both these cases the levels are normally well separated in energy; postcollision interaction (PCI) between the slow scattered projectile and the ejected electron causes overlap via substantial shifts and broadening of the levels.[3]

Although these are true examples of coherent excitation, in multielectron atoms many closely spaced autoionizing levels naturally overlap, and coherence effects do not depend on PCI. Here we report such effects observed using $(e,2e)$ spectroscopy on a cadmium target, with the relatively high electron-impact energy of 150 eV.

The most prominent feature in the Cd ejected-electron spectrum is the broad $4d^9 5s^2 5p\ ^1P_1$ autoionizing line profile at an ejected-electron energy of 3.81 eV.[4] In previous work[5] we measured $(e,2e)$ ejected-electron angular distributions at this energy, for a range of scattering angles 2.5°–8.5° and an incident energy of 150 eV. Each angular distribution had maxima for directions parallel and antiparallel to the momentum-transfer vector; these features are known as the binary and recoil peaks, respectively. It was found that the binary- to recoil-peak intensity ratio increased with scattering angle, which implied the existence of interference terms caused by the coherent population of $J\neq 1$ continua and the (resonantly populated) $J=1$ continuum. An analysis of the data showed that the magnitude of the interference terms cannot be accounted for by the direct ionization process alone, but requires the existence of $J\neq 1$ autoionizing levels that overlap the $J=1$ level.

We have begun our investigation into these phenomena by measuring $(e,2e)$ spectra for a scattering angle of 3°. The reason for choosing this relatively small angle, for which the interference effects due to coherent excitation are small and difficult to observe, is that it enables us to construct a simple model (Sec. II) for the interpretation of the experimental results presented in Sec. IV.

II. THEORY

A. Cadmium $(e,2e)$ angular distributions

The nominal ground-state configuration of cadmium is $(4d^{10}5s^2)\ ^1S_0$, but there is significant configuration interaction[6] and the outermost subshell includes 6% $5p^2$. This is of importance here since we are interested in the coherent excitation, by electron impact, of the odd-parity $4d^9 5s^2 5p\ J=1$ and even-parity $4d^{10}5pnp\ J=0,2$ $(n=5,6,7)$ series of autoionizing levels. Both these types of configurations can be populated from the ground state by single electron promotion, the first by $4d\rightarrow 5p$ and the second by $5p\rightarrow np$; autoionization occurs via configuration interaction with the $5sEp$ and $5sEs,Ed$ continua, respectively, since only the ground-state ion Cd^+ $(5s)\ ^2S_{1/2}$ is energetically accessible from these autoionizing levels.[7] The corresponding *direct* ionization processes are $5s^2\rightarrow 5sEp$ and $5s^2\rightarrow 5sEs,Ed$.

The significant spin-orbit energies of the cadmium outer-subshell electrons result in autoionizing levels that are examples of intermediate coupling.[8] For example, in an LS basis the three $4d^9 5s^2 5p\ J=1$ levels are each admixtures of $^1P_1$, $^3P_1$, and $^3D_1$. Nonexchange electron-impact excitation of all three levels is then determined by the dipole matrix element for $^1S_0 \rightarrow {}^1P_1$. Autoionization, however, can take place from both the $^1P_1$ and $^3P_1$ components into the corresponding singlet and triplet continua; from parity considerations the $^3D_1$ component is inactive. In general, any Cd autoionizing level belonging to a configuration with two nonequivalent electrons outside closed shells (or hole plus electron) may be excited by a non-exchange-multipole transition via its ^1L_J component, and may autoionize into $5sEl\,{}^{2S+1}L_J$ continua, where $l=L=J$ and $S=0$ or 1.

In the $(e,2e)$ experiments the ion and ejected-electron spin are unobserved. In the formalism of angular-momentum-transfer theory,[9] autoionization into the singlet continuum is a parity-favored process with angular-momentum transfer $j_t=0$, whereas autoionization into the triplet continuum is a parity *un*favored process with $j_t=1$. The angular distribution of ejected electrons, observed in coincidence with incident electrons scattered through θ_{sc}, is then given by a coherent sum over J but an *in*coherent sum over j_t. In the present case $j_t=S$ and this incoherence follows immediately from the integration over the unobserved reactants; i.e., $\langle S'M_S'|SM_S\rangle=\delta_{S'S}\delta_{M_S'M_S}$, so cross-terms between different spin states vanish.

Then, following coherent excitation of a number of autoionizing levels, the general form of the angular distribution of electrons ejected with energy E at angle (θ_{ej},ϕ_{ej}), measured in coincidence with electrons scattered through an angle θ_{sc}, may be written[10]

$$I(\theta_{sc};E;\theta_{ej},\phi_{ej}) \sim \sum_{SM_S} \left| \sum_{\gamma JM} \alpha_{\gamma JM}(\theta_{sc})\, A_{\gamma JS}(E) \langle JS(M-M_S)M_S|JSJM\rangle\, Y_{J(M-M_S)}(\theta_{ej},\phi_{ej}) \right|^2 , \tag{1}$$

where Y_{lm} are spherical harmonics, and a Clebsch-Gordan coefficient has been used to uncouple the unobserved spin from the orbital angular momentum of the ejected electron. In the independent-particle model used here, γ is a label that distinguishes different configurations giving rise to the same value of J. The $a_{\gamma JM}$ are the complex excitation amplitudes of $\gamma\,{}^1L_J$ $(L=J)$. The phase and amplitudes of these coefficients depend strongly on scattering angle, but, in the independent-particle approximation, are independent of E since they refer to discrete configurations. The $A_{\gamma JS}$ are complex coefficients that depend on the atomic autoionizing process but are independent of the scattering process. Both the magnitudes and phases of these coefficients are rapidly varying functions of E through their dependence on the autoionization phase parameter[11] Δ_{JS}. (For a single level, of width Γ_J and centered on E_J, coupled to a single continuum, $\Delta_{JS}=-\arctan[\frac{1}{2}\Gamma_J/(E-E_J)]$ and $|A_{JS}| \propto \sin\Delta_{JS} - \cos\Delta_{JS}/q_J$. Here q_J is analogous to the Fano-Beutler asymmetry parameter,[11] but is in general a *complex* quantity which allows for a phase difference between the electron-impact amplitudes for the resonant and direct ionization processes.) The phase of $A_{\gamma JS}$ is given by the asymptotic form of the ejected-electron wave function at large radii:[11,12]

$$\psi_{e^-} \sim \sin(kr+\delta_{JS}^T) , \tag{2}$$

with

$$\delta_{JS}^T = -\tfrac{1}{2}J\pi + \sigma_J + \delta_{JS} + \Delta_{JS} , \tag{3}$$

where k is the electron momentum, σ_J is the hydrogenic Coulomb phase, and δ_{JS} is the phase shift due to the unperturbed non-Coulombic ionic potential. Both these quantities are slowly varying functions of E. Note that the phase shift due to autoionization, Δ_{JS}, is the net shift due to all configurations γ that couple to the same continua.

B. Plane-wave Born-approximation limit

The $(e,2e)$ experiments reported below were carried out in Cd for an incident electron energy of 150 eV, $\theta_{sc}=3°$, and $E=2.6$–4.8 eV. Previous work[13] has shown that under these conditions the plane-wave Born approximation (PWBA) is valid, in which case Eq. (1) may be simplified by choosing the quantization axis along the direction of momentum transfer $\mathbf{K}$, and thus $M=0$ only. Also, in the PWBA limit, the relative phase of the $a_{\gamma J0}$ is given by the factor[14] i^J. Then, coplanar measurements (i.e., $\phi_{ej}=0$) at $\theta_{ej}=\theta_K$ and $\theta_K+180°$ (i.e., along $\pm\mathbf{K}$), which vary E and the corresponding scattered electron energy, yield $(e,2e)$ energy spectra:

$$I^{\pm}(3°;E) \sim \sum_{\gamma J\gamma' J'} (\pm 1)^{J+J'} ([J][J'])^{1/2} |a_{\gamma J0} A_{\gamma J0}|\, |a_{\gamma' J'0} A_{\gamma' J'0}| \cos[\delta_{J0}^T - \delta_{J'0}^T + \tfrac{1}{2}\pi(J-J')] , \tag{4}$$

where $[j]=2j+1$ and we have omitted constants common to all terms. The argument of the cosine is the relative phase due to both excitation and autoionization. Only parity-favored $(S=0)$ terms are present; all parity-unfavored terms $(S=1)$ vanish because (a) $Y_{lm}(0,0)=0$ if $m\neq 0$, and (b) $\langle J100|J1J0\rangle=0$ since $J+1+J$ is odd.[15]

The factor $(\pm 1)^{J+J'}$ occurs because Y_{J0} changes sign for J odd when $\theta_{ej}\rightarrow\theta_{ej}+180°$. Thus cross-terms with

$J+J'$ odd lead to different magnitudes of the binary and recoil peaks in $(e,2e)$ ejected-electron angular distributions.[16]

We now make the assumption that, for our experimental conditions, the multipole excitation amplitudes for $J \geq 3$ may be neglected, and of the remaining amplitudes, the dipole process ($J=1$) dominates. Thus, we also neglect the product of two small amplitudes and obtain the relationships

$$(I^+ + I^-) \sim 6|a_{10} A_{10}|^2 , \tag{5}$$

$$(I^+ - I^-) \sim 4\sqrt{3}|a_{10} A_{10}| \sum_{J}^{0,2} [J]^{1/2} \sum_{\gamma} |a_{\gamma J0} A_{\gamma J0}| \cos[\delta_{10}^T - \delta_{J0}^T + \tfrac{1}{2}\pi(1-J)] , \tag{6}$$

where, because the dipole-allowed spectrum is dominated by the $4d^9 5s^2 5p$ configuration, we have dropped the label γ from the $J=1$ terms.

Thus, manipulation of $(e,2e)$ spectra taken along $\pm\mathbf{K}$ enables different terms to be isolated. The summed spectrum $(I^+ + I^-)$ strips off the cross-terms to yield the parity-favored part of the dipole process, whereas the difference spectrum $(I^+ - I^-)$ reveals the interference cross-terms caused by the coherent excitation of overlapping autoionizing levels.

C. Calculation of the sum and difference spectra

We wish to calculate the $A_{\gamma J0}$ for the range $E=2.6$–4.8 eV. In order to obtain numerical estimates that contain the minimum number of arbitrary parameters to be fitted to the experiment, we shall make a number of assumptions and approximations in what follows. The single most important of these is that any matrix elements used in the calculation are independent of energy over the range of interest.

The positions and widths of the $4d^9 5s^2 5p$ $J=1$ levels that dominate this spectral region are well known from photoabsorption spectroscopy,[17,18] but those of the optically forbidden even-parity levels are uncertain. Available *ab initio* calculations of positions[19] and widths[20] show that we need to consider the $5pnp$ ($n=5,6,7$) $J=0,2$ levels.

The $J=0$ levels of $5pnp$ (positions E_{nr} and widths Γ_{nr}, where $r=1,2$) may be expressed in terms of LS-coupled basis functions as $|nr0\rangle = \sum_b c_{nrb}|b\rangle$, where $b=1$ denotes ^1S and $b=2$ denotes ^3P. Excitation from the ground state occurs via the singlet component of each level and the excitation amplitudes may therefore we written $c_{nr1}|a_{n00}|$. [Notice that the definition of $a_{\gamma JM}$ anticipated this result; the label γ refers to a *configuration* (here $\gamma \equiv n$) rather than an individual level n,r; the coefficients c_{nr1} are then incorporated in the A_{n00}.] Each level couples to the single continuum $5sEs\ ^1S_0$ to produce a width $\Gamma_{nr} = \pi|v_{nr}|^2$ via the matrix element $v_{nr} = c_{nr1} V_n$, where $V_n = \langle 5pnp\ ^1S_0|V|5sEs\ ^1S_0\rangle$. Thus, for each level *within* a configuration, the ratio of the excitation matrix element to that for autoionization is given by $|a_{n00}|/V_n$, and is independent of r. We now make the assumption that the value of this ratio is the same for each of the three configurations $n=5,6,7$. This is true for the upper members of a well-behaved Rydberg series, where wavefunction normalization leads to the same n scaling for excitation and autoionization matrix elements (and also that for direct ionization),[11] but is probably not a good approximation here. However, we employ the scaling because it enables us to eliminate two of the three unknown a_{n00} by using the *ab initio* V_n ratios. We choose to keep the $n=6$ amplitude since this configuration has the largest energy overlap with the $J=1$ levels. Then $|a_{n00}| = (V_n/V_6)|a_{600}|$. Using the theory of a number of discrete states coupled to a single continuum,[11] we then obtain

$$\tan\Delta_{00} = -\sum_{n,r} \frac{\Gamma_{nr}}{E - E_{nr}} \tag{7}$$

and

$$\sum_n |a_{n00} A_{n00}| = \frac{|a_{600}|}{\pi V_6} (\sin\Delta_{00} - \cos\Delta_{00}/q_0) . \tag{8}$$

Thus, because of our n-scaling assumption, Eq. (8) has exactly the same form as the isolated resonance case,[11] but with the phase shift due to autoionization given by Eq. (7).

The $J=2$ levels of $5p^2$ are admixtures of ^3P, ^1D and those of $5p6p, 5p7p$ are admixtures of ^3P, ^1D and ^3D. Thus $5p^2$ only couples to the $5sEd\ ^1D_2$ continuum, whereas the other configurations can, in addition, couple to the $^3D_2$ continuum. However, the *ab initio* calculations[20] show that the coupling to this latter coupling is very weak and can, to a good approximation, be ignored. Thus, with our scaling assumption, we use Eqs. (7) and (8) with $J=2$ and the single excitation amplitude a_{620}.

The number of unknown parameters may be reduced by establishing an approximate relationship between $|a_{600}|$ and $|a_{620}|$. The PWBA calculation involves known angular factors and a radial integral in a spherical Bessel function of order J for electron promotion,[21] $\int P_{6p}(r) j_J(Kr) P_{5p}(r) dr$. For our experimental conditions the momentum transfer K is 0.2 Bohr radii. Assuming that the largest contribution to the integral is from the radial region where Kr is small, we expand the Bessel function in the integrand[21] and obtain, to first order, $j_0 \approx 1-(Kr)^2/4$, where the integral over the first term vanishes since the P_{nl} are orthogonal, and $j_2 \approx (Kr)^2/15$. Combining this result with the angular factors we finally obtain

$$\frac{|a_{600}|}{|a_{620}|} \approx \frac{1}{\sqrt{2}} \frac{15}{4} . \tag{9}$$

The three $4d^9 5s^2 5p\ J=1$ levels couple strongly to both the singlet and triplet continua.[22] The theory of several levels interacting with two continua[23] and its application to this configuration has been described elsewhere;[24] only an outline is given here. The discrete-continuum interaction replaces the two unperturbed $S=0,1$ continua with two new orthogonal energy-dependent wave functions Ψ^+ and Ψ^-, each admixtures of singlet and triplet continua and prediagonalized discrete states. The $J=1$ component of the final state following dipole excitation (d) from the ground state (γ_0) is then

$$\Psi^{(d)} \propto \Psi^+ \langle \Psi^+ | d | \gamma_0 \rangle + \Psi^- \langle \Psi^- | d | \gamma_0 \rangle . \tag{10}$$

The matrix elements are proportional to the $^1P_1$ components of $\Psi^{\pm}$; the excitation amplitude $|a_{10}|$ may therefore be factored out in Eq. (10). Grouping the asymptotic form ($r_{Ep} \to \infty$) of $\Psi^{(d)}$ into singlet and triplet terms then yields expressions for $|A_{10}|$ and Δ_{10}.

We are now in a position to calculate $|A_{\gamma J0}|$ and Δ_{J0} for $J=0,1,2$. The necessary input parameters for $J=0,2$ are obtained from the *ab initio* calculations[19,20] and those for $J=1$ are taken from the analysis in Refs. 24 and 25 of the experimental photoabsorption cross section. Table I lists the energies and widths of the levels. To complete the calculation of the sum and difference spectra [Eqs. (5) and (6)], we require the J dependence of the phases σ_J and δ_{J0}. Those of the former are readily found from the properties of Coulomb functions:[26]

$$\sigma_{J+1} - \sigma_J = -\arctan\left[\frac{1}{J+1}\frac{1}{\sqrt{E}}\right] , \tag{11}$$

where E is in Ry. Estimates of δ_{J0} may be found by extrapolating the quantum defect behavior of $5snl$ ($l=J$) Rydberg series across the ionization potential. The available spectroscopic data[7,27] for $L=0,1,2$ show that all these quantum defects are n independent (except for the lowest members of each series) to within ± 0.02. Furthermore, this small variation is randomly distributed and thus appears to be due to experimental error rather than any systematic trend as n increases. We have therefore taken δ_{J0} to be independent of energy from threshold to the ejected-electron energy range of interest, and we obtain

$$\delta_{10} - \delta_{20} = 0.83\pi \quad \text{and} \quad \delta_{10} - \delta_{00} = -0.56\pi . \tag{12}$$

The uncertainty of 0.02π ($=4°$) has negligible effect on our calculations.

Figures 1 and 2 show the calculated interference terms in $I^+ - I^-$ separately for $(J=1)\times(J=0)$ and $(J=1)\times(J=2)$, respectively. To illustrate the effect of overlapping autoionizing levels, the solid lines assume that direct ionization is negligible for $J=0,1,2$ (i.e., $q_J = \infty$); this is experimentally true for $J=1$.[18,24] The vertical scales are arbitrary, except that the relative scales of the two figures are given by Eq. (9). The dotted curves correspond to $J=1$ autoionization, but *only* direct ionization for $J=0,2$, i.e., $\Delta_{J0}=0$ and $|A_{6J0}| = \text{const}$, where the values of the constants have been arbitrarily chosen to make the curves equal the solid curves at the $^1P_1$ interference maxima.

The two curves in Fig. 1 are similar in the region of the $^3P_1$ resonance because this resonance lies in the high-energy tail of the broadest of the $J=0$ resonances, which acts as a quasicontinuum. The equivalent is true in Fig. 2, except that the solid line is inverted because the discrete-continuum matrix elements for $J=2$ and 0 differ in sign.[20] The greatest difference between the solid and dotted curves in both cases occurs in the region just

TABLE I. Cd autoionizing level energies (above the ionization potential) and widths used in our calculations. The $J=1$ values are from photoabsorption data (Refs. 18 and 24). The $J=0,2$ energies are from Ref. 19 and their widths are from Ref. 20).

			Energy (eV)	Width (eV)
$J=0$	$5p^2$	^1S	1.94	0.184
	$5p6p$	^3P	3.69	0.0007
		^1S	4.19	0.006
	$5p7p$	^3P	4.49	0.0007
		^1S	4.77	0.006
$J=1$	$4d^9 5s^2 5p$	^3P	3.07	0.041
		^1P	3.81	0.140
		^3D	3.94	0.003
$J=2$	$5p^2$	^1D	0.88	1.1
	$5p6p$	^3D	3.50	0.013
		^3P	3.89	0.023
		^1D	4.02	0.137
	$5p7p$	^3D	4.42	0.026
		^3P	4.71	0.012
		^1D	4.81	0.098

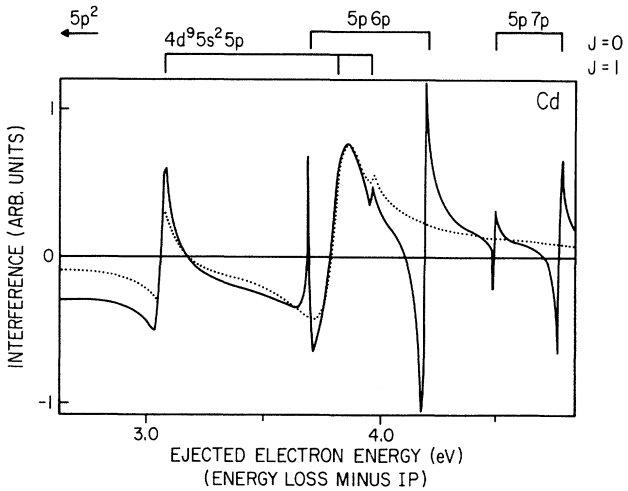

FIG. 1. Calculated $(J=0)\times(J=1)$ contribution to the interference spectrum given by Eq. (6). The solid line assumes only autoionization, and the dotted line assumes only direct ionization for $J=0$.

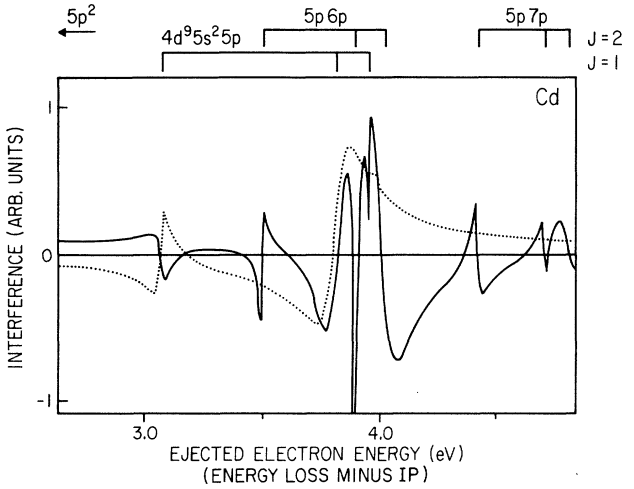

FIG. 2. As Fig. 1 (with the same vertical scale), but for $(J=1)\times(J=2)$.

above the $^1P_1$ resonance. The highest $5p6p$ $J=0,2$ levels cause the interference terms to be negative, whereas for the direct ionization case they remain positive.

III. EXPERIMENT

The experiments were carried out using a coplanar $(e,2e)$ spectrometer which has been described previously.[5] It consists of four main components: an electron gun, a metal-vapor atomic-beam oven, a scattered-electron spectrometer, and an ejected-electron spectrometer (Fig. 3). The electron gun is recessed in a sidearm of the vacuum chamber, which enables the ejected-electron spectrometer to be positioned on both sides of the electron-beam axis. Thus spectra for two ejected-electron angles 180° apart may be taken in a single experimental run at the same value of θ_{sc}. The coincidence count rate was fairly low (2 s^{-1} in the $^1P_1$ peak) and long run times are required for acceptable statistics in the difference between two spectra. To minimize the effect of any drift in the experimental parameters (electron beam, cadmium beam, detector efficiency, etc.) energies and angles are scanned sequentially in the following manner. With the ejected-electron detector set at $\theta_{ej}=\theta_K$, the energy is scanned over the desired range (5 s at each of 110 steps in the present experiment). A stepping motor then rotates the detector to $\theta_K+180°$, where the energy scan is repeated. The detector is then rotated back to θ_K for the start of the next sequence. The data presented below are the result of a continuous experimental run lasting 11 days.

Our data analysis involves the subtraction of two nearly identical $(e,2e)$ spectra and great care has to be taken to ensure correct alignment of the two energy scales. Misalignment can occur because small residual magnetic fields (in our case a few mG) noticeably affect the pass energy of hemispherical electrostatic energy analyzers when $\theta_{ej}\rightarrow\theta_{ej}+180°$. The effect of misalignment is to distort the interference spectrum by introducing a component which is the *derivative* with respect to energy of the nearly identical spectra: $I(E+\delta E)-I(E)\approx(dI/dE)\delta E$, which is proportional to the alignment error δE. Aligning the scales by using the maxima in the two $(e,2e)$ spec-

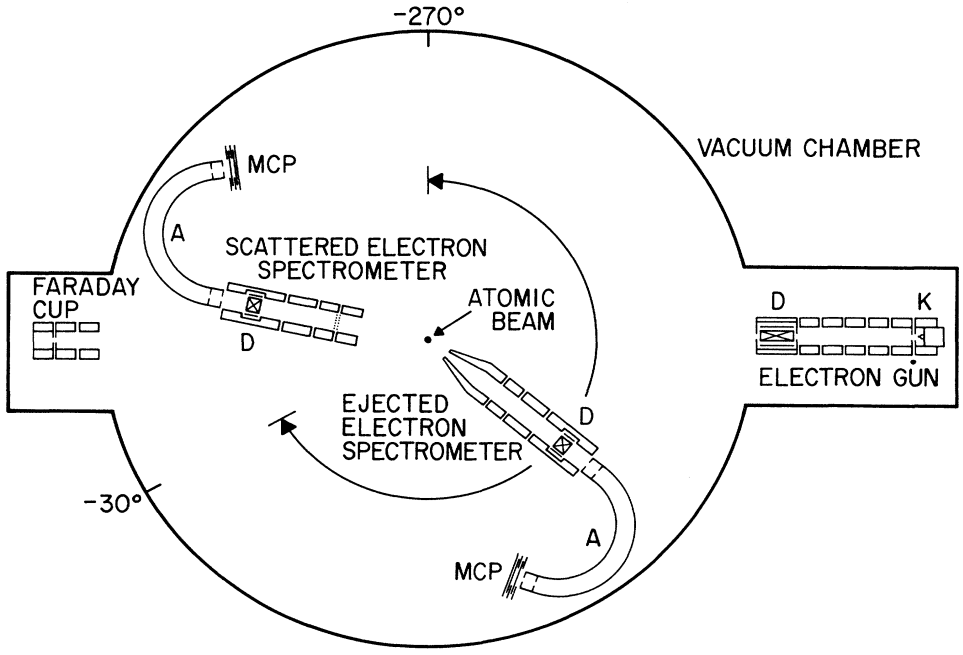

FIG. 3. The $(e,2e)$ spectrometer. K, cathode; D, deflector; A, hemispherical-sector electrostatic analyzer; MCP, microchannel-plate electron detector.

tra is not necessarily appropriate since interference effects could cause significant shifts from their natural positions. In the present case the energy scales were aligned by examining the noncoincident ejected-electron energy spectra due to the random part of the coincidence counts that lay outside the true coincidence time window. (These spectra are, in fact, the product of the scattered and ejected count rates; since the energy resolution of the scattered detector was set to ~ 0.5 eV, we actually obtain an ejected-electron spectrum modulated by a broad envelope.) Since these ejected-electron spectra are uncorrelated with scattering angle, interference effects due to coherent excitation are, to some extent, averaged out. By using the $J=1$ resonance positions we believe we have aligned the two spectra to better than 5 meV.

IV. RESULTS AND DISCUSSION

Figure 4 shows $(e,2e)$ spectra for $\theta_{sc}=+3°$ and $\theta_{ej}=-50°$ and $-230°$ (i.e., along $\pm\mathbf{K}$ to obtain $I^{\pm}$), for an incident electron energy of 150 eV. The spectral range is $E=2.6$–4.8 eV with corresponding scattered-electron energy 138.41–136.21 eV, since the ionization potential of cadmium is 8.99 eV.[7] Small differences in the spectra can be seen; most obvious of these are the different widths at the base of the main peak. Figure 5 is the sum of these two spectra. The statistical uncertainties are approximately the same as the size of the data points in the figure. The summed spectrum was used both to calibrate the energy resolution of the apparatus and to test our calculated $|A_{10}|^2$. The solid curve is thus the parity-favored part of the dipole excitation cross section [Eq. (5)] folded with a Gaussian of full width at half maximum (FWHM) 0.15 eV, and normalized to the data in the main peak. Agreement with the data is satisfactory in that the relative intensity of the singlet and triplet resonances is correctly predicted and our neglect of small terms in Eq. (5) appears to be justified.

Figure 6 is the difference between the two spectra of Fig. 4. In order to improve the statistics the data shown have been smoothed by simple three-point averaging. The vertical scales in Figs. 5 and 6 differ by a factor of 30, which is a measure of the interference contribution to the total signal. The solid line is the calculated $I^{+}-I^{-}$, assuming no direct ionization (the sum of Figs. 1 and 2), folded with a Gaussian of 0.15 eV FWHM. Considering the approximations and assumptions we have made in the calculations, the agreement with experiment is remarkably good; the *only* adjustable parameter is the overall normalization constant. Quantitatively, the agreement is best in the $^1P_1$ resonance region. Provided that Eq. (9) is valid, we can extract PWBA amplitude ratios from the experiment. From Figs. 5 and 6 we find

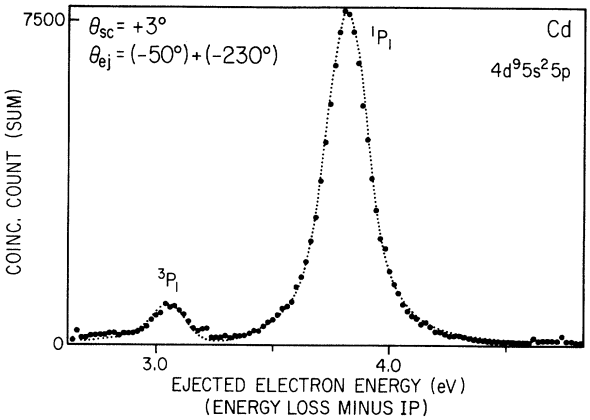

FIG. 5. The sum of the two spectra in Fig. 3. The statistical errors are about the same size as the data points. The dotted line is the calculated parity-favored $J=1$ spectrum, folded with a Gaussian of 0.15 eV FWHM and normalized to the data.

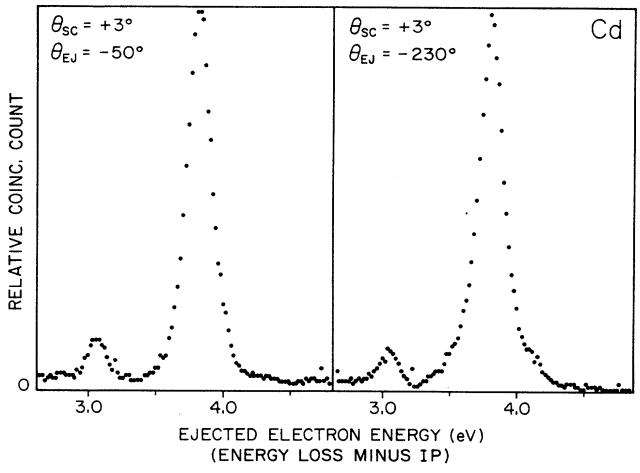

FIG. 4. Coincidence spectra for $\theta_{ej}=-50°$ (binary peak) and $-230°$ (recoil peak), with $\theta_{sc}=+3°$, 150 eV incident energy.

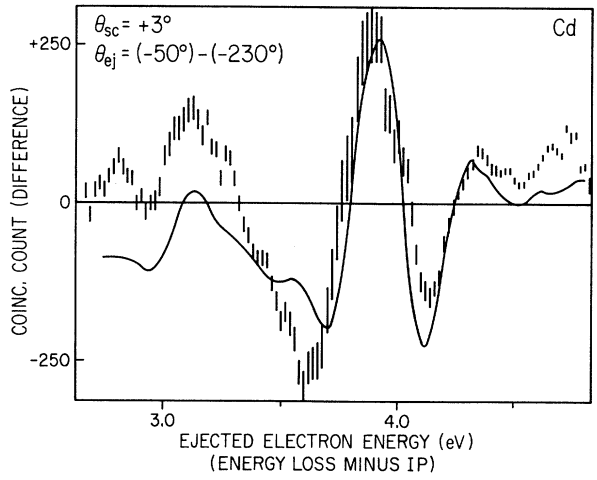

FIG. 6. The difference between the two spectra in Fig. 3. The data have been smoothed with simple three-point averaging. The solid line is the calculation described in the text, folded with a Gaussian of 0.15 eV FWHM and normalized to the data in the main positive peak.

$$\frac{|a_{600}|}{|a_{10}|}=\frac{|\langle {}^1S_0|e^{i\mathbf{K}\cdot\mathbf{r}}|{}^1S_0\rangle|}{|\langle {}^1P_1|e^{i\mathbf{K}\cdot\mathbf{r}}|{}^1S_0\rangle|}=0.21$$

and

$$\frac{|a_{620}|}{|a_{10}|}=\frac{|\langle {}^1D_2|e^{i\mathbf{K}\cdot\mathbf{r}}|{}^1S_0\rangle|}{|\langle {}^1P_1|e^{i\mathbf{K}\cdot\mathbf{r}}|{}^1S_0\rangle|}=0.08\ ,$$

where the matrix elements are between the ground state and the singlet basis states of the discrete configurations.

Qualitatively, there is excellent agreement between the calculated curve and the data. The experimental positions of the various maxima and minima are faithfully reproduced by the theory; the minimum just above 4.0 eV is clear evidence that direct $J=0,2$ ionization is, on its own (see Figs. 1 and 2), unable to explain the data. Notice, in particular, the point of inflection in the theoretical curve at 3.5 eV due to the lowest $5p6p\ J=2$ level (see Fig. 2). This corresponds to a similar point of inflection in the data at 0.08 eV lower energy. We have seen this feature in three separate experiments and therefore believe it to be real, in which case we may make the assignment

$$E(5p6p\ {}^3D_2)=3.42\pm0.02\ \text{eV}\ .$$

This is the only previously undetected level that we can assign; the interference features above 4.0 eV consist of the smoothed-out contributions from many $J=0,2$ levels.

The largest quantitative discrepancy occurs in the $^3P_1$ region of Fig. 6, where, although the calculated *shape* agrees with the data, theory and experiment are vertically offset. This disagreement is presumably due to the large number of approximations and assumptions made in our calculation. However, we are unable to improve the overall agreement either by introducing direct $J=0,2$ ionization or by varying the $|a_{600}|/|a_{620}|$ value from that given by Eq. (9). The most likely source of error in our calculations is n scaling applied to $5p^2$, which is the configuration primarily responsible for the interference spectrum at low energies.

One effect that we have omitted from our calculation, which may provide a possible explanation of the discrepancies, is postcollision interaction (PCI) between the scattered and ejected electrons. It is known from ion-atom–collision calculations that PCI can produce substantial shifts and broadenings (accompanied by distortion) of natural autoionizing line profiles, even at ion velocities comparable to those of the scattered electrons in our experiment.[28] The magnitude of these effects is approximately proportional to the natural width and is also strongly dependent on the ejected-electron direction. In addition (and of particular relevance here), the phase shift across a resonance can increase by substantially more than the natural value of π. Clearly, PCI effects would manifest themselves most strongly for the very broad (1.1 eV) $5p^2\,{}^1D_2$ level, which is responsible for the low-energy $J=2$ contribution to the interference spectrum.

V. CONCLUSIONS

We have observed interference effects in $(e,2e)$ spectra in Cd due to the coherent excitation of a number of overlapping autoionizing resonances. The experimental results are in quite good agreement with calculations, but there are noticeable discrepancies. *Ab initio* values of PWBA matrix elements for all the discrete configurations and continua would be helpful and would enable a calculation of the interference spectrum containing *no* arbitrary parameters. The calculation of PCI effects for the present system is also desirable. In future experiments we intend to investigate the <2-eV region of the spectrum in order to find the previously undetected $5p^2\,{}^1D_2$ level. Since this level is expected to be very broad, a direct measurement of PCI effects as a function of ejected-electron angle may be possible.

At present, experiments are underway to repeat the type of measurement described in this paper, but at larger scattering angles. Preliminary results indicate that the difference between the $\pm\mathbf{K}$ spectra increases, over the entire spectral range investigated, with scattering angle; i.e., the $(J=0,2)/(J=1)$ amplitude ratios increase, and therefore the interference terms become more important. Analysis of the data is more complicated than in the present case, since the breakdown of the PWBA not only allows the population of states $|M|>0$, but also introduces changes in the relative phases of the excitation amplitudes.

ACKNOWLEDGMENTS

We wish to thank Dr. M. Wilson for carrying out the calculations of the $J=0,2$ level widths.

[1]N. Anderson, J. W. Gallagher, and I. V. Hertel, Phys. Rep. **165**, 1 (1988).

[2]P. van der Straten and R. Morgenstern, Comments At. Mol. Phys. **17**, 243 (1986).

[3]R. Morgenstern, A. Niehaus, and U. Thielmann, J. Phys. B **10**, 1039 (1977).

[4]V. Pejčev, K. J. Ross, D. Rassi, and T. W. Ottley, J. Phys. B **10**, 459 (1977).

[5]N. L. S. Martin and D. B. Thompson, J. Phys. B (to be published).

[6]J. E. Hansen, Phys. Rev. A **15**, 810 (1977).

[7]C. E. Moore, *Atomic Energy Levels,* Natl. Bur. Stand. (U.S.) Circ. No. 467 (U.S. GPO, Washington, D.C., 1958), Vol. III.

[8]M. Wilson, J. Phys. B **1**, 736 (1968).

[9]U. Fano and D. Dill, Phys. Rev. A **6**, 185 (1972); D. Dill, *ibid.* **7**, 1976 (1973).

[10]This equation is an extension of Eq. (5) of Ref. 2 to cover the case of intermediate coupling.

[11]U. Fano. Phys. Rev. **124**, 1866 (1961).

[12]H. A. Bethe and E. E. Salpeter, *Quantum Mechanics of One- and Two-Electron Atoms* (Springer, Berlin, 1957), p. 22; there is an erratum in Eq. (4.10): the term in σ_l should be positive.

[13]N. L. S. Martin, T. W. Ottley, and K. J. Ross, J. Phys. B **13**, 1867 (1980); see also V. V. Balashov, E. G. Berezhko, A. N. Grum-Grzhimailo, N. M. Kabachnik, and A. I. Magunov, *ibid.* **13**, L269 (1980).

[14]N. F. Mott and H. S. W. Massey, *The Theory of Atomic Collisions,* 3rd ed. (Clarendon, Oxford, 1965), p. 22.

[15]See, for example, A. R. Edmonds, *Angular Momentum in Quantum Mechanics* (Princeton University Press, Princeton, 1957).

[16]S. T. Manson, L. H. Toburen, D. H. Madison, and N. Stolterfoht, Phys. Rev. A **12**, 60 (1975).

[17]J. Berkowitz and C. Lifshitz, J. Phys. B **1**, 438 (1968).

[18]G. V. Marr and J. M. Austin, Proc. R. Soc. London, Ser. A **310**, 137 (1969).

[19]M. W. D. Mansfield and M. M. Murnane, J. Phys. B **18**, 4223 (1985). The fitted $5p6p$ and $5p7p$ configuration-average energies given in this reference are based on tentative assignments. The values we have used were obtained by fixing the $5pnp$ ($n=5,6,7$) configuration separation at the *ab initio* values, and then using the fitted $5p^2$ configuration-average energy. Thus the values in Table I of our paper are 0.21 eV lower than those given in this reference.

[20]M. Wilson (private communication).

[21]R. D. Cowan, *The Theory of Atomic Structure and Spectra* (University of California Press, Berkeley, 1981), Sec. 18-12.

[22]N. L. S. Martin, Nucl. Instrum. Methods B **40/41**, 228 (1989).

[23]E. B. Saloman, J. W. Cooper, and D. E. Kelleher, Phys. Rev. Lett. **55**, 193 (1985); D. E. Kelleher, in *Proceedings of the 5th International Conference on Spectral Line Shapes,* edited by B. Wende (de Gruyter, Berlin, 1981), p. 281, and private communication.

[24]N. L. S. Martin, J. Phys. B **23**, 2223 (1990).

[25]N. L. S. Martin, J. Phys. B **17**, 1797 (1984).

[26]M. Abramowitz and I. A. Stegun, *Handbook of Mathematical Functions* (Dover, New York, 1970), p. 540.

[27]C. M. Brown and S. G. Tilford, J. Opt. Soc. Am. **65**, 1404 (1975).

[28]P. van der Straten and R. Morgenstern, J. Phys. B **19**, 1361 (1986).